Elemental and Isotopic Fractionation in ^{3}He-rich Solar Energetic Particle Events

M. E. Wiedenbeck*, R. A. Leske†, C. M. S. Cohen†, A. C. Cummings†, R. A. Mewaldt†, E. C. Stone† and T. T. von Rosenvinge**

*Jet Propulsion Laboratory, California Institute of Technology, Pasadena, CA 91109
†California Institute of Technology, Pasadena, CA 91125
**NASA Goddard Space Flight Center, Greenbelt, MD 20771

Abstract. Using data from the Solar Isotope Spectrometer (SIS) on the Advanced Composition Explorer (ACE) mission, heavy ion composition measurements have been made in 26 ^{3}He-rich solar energetic particle (SEP) events that occurred between 1998 and 2004. Relative abundances of 13 elements from C through Ni have been investigated, as have the isotopic compositions of the elements Ne and Mg. We find a general tendency for the abundances to follow trends similar to those found in gradual SEP events, in which fractionation can be represented in the form of a power-law in Q/M. However several deviations from this pattern are noted that may provide useful diagnostics of the acceleration process occurring in solar flares.

Keywords: solar energetic particles, solar flares, composition, isotopes
PACS: 96.50.Vg, 96.50.sb, 96.50.Pw

INTRODUCTION

Characteristics of impulsive (^{3}He-rich) solar energetic particle events have been extensively studied and are summarized in various review articles [1, 2]. In addition to the enhancement of the ^{3}He/^{4}He ratio by several orders of magnitude over the solar wind value of $\sim 5 \times 10^{-4}$, which is commonly used for identifying such events, other compositional signatures are well established. In particular, heavy element abundances increase approximately monotonically with atomic number, Z, such that Fe/O ratio is typically enhanced by a factor of nearly 10 over the solar wind value of ~ 0.12 [3]. This trend has recently been shown to extend to the heaviest elements [4, 5].

Models for the origin of the compositional features of ^{3}He-rich events are faced with the need to simultaneously account for two facts that are seemingly contradictory. On the one hand, enhancements of elemental abundances exhibit a relatively smooth variation with mass-to-charge ratio (Q/M, estimated based Z and an assumed source region temperature of a few$\times 10^6$ K). The Q/M values over which this trend is observed vary by a factor $\sim$1.5–2 from O to Fe and another factor $\sim$3 from Fe to the heaviest elements [6]. On the other hand, ^{3}He is enhanced with a high degree of selectivity relative to ^{4}He, in spite of the fact that their Q/M values differ only by a factor 4/3, that is, much less than the variation among the elements. Furthermore, enhancements of ^{3}He/^{4}He can be a factor of 10^3 or greater while Fe/O is typically enhanced by a factor $\sim$10. Most composition-related theoretical work to date has focused on accounting for either the ^{3}He enhancement or the heavy-ion enhancements, not both.

CP1039, *Particle Acceleration and Transport in the Heliosphere and Beyond— 7th Annual Astrophysics Conference*
edited by G. Li, Q. Hu, O. Verkhoglyadova, G. P. Zank, R. P. Lin, and J. Luhmann

Here we use heavy ion data in the energy range 12–60 MeV/nuc from the SIS instrument on ACE to investigate compositional trends in ^{3}He-rich SEP events. Although SIS detected more than 100 ^{3}He-rich events during solar cycle 23, only 26 of these events had high enough intensities of $Z \geq 6$ elements to be used for this study.

ISOTOPIC COMPOSITION

The SIS instrument [7] uses the dE/dx versus total energy technique to determine the nuclear charge, Z, and, in some cases, the mass, M, of energetic particles that stop in a stack of silicon solid state detectors. The resolution improves as the number of detectors penetrated (the particle "range") increases, but for the typically soft energy spectra encountered in ^{3}He-rich events, the bulk of the detected particles have short ranges. Figure 1 shows mass histograms for Ne and Mg in two different range intervals from the most intense of the 26 events studied (20 Aug 2002), which yielded more than twice the amount of Ne and Mg as detected in the other 25 events combined. Summing the data from those other 25 events yields mass histograms having similar resolution to those shown in Figure 1. The dotted lines on the histograms indicate how the mass distributions were split up to obtain abundances of ^{20}Ne, ^{22}Ne, ^{24}Mg, and ^{26}Mg. Since the solar wind abundance of ^{21}Ne is low (^{21}Ne/Ne$\simeq$0.002, [3]), its contribution to the derived abundances of the two more-abundant isotopes is negligible. However, ^{25}Mg/Mg$\simeq$0.1 in the solar wind, so the effects of contamination of the ^{24}Mg and, particularly, the ^{26}Mg abundance with some ^{25}Mg must be considered.

Since the work of Breneman and Stone [8], it has been known that in large, gradual SEP events there is elemental fractionation relative to coronal or solar wind abundances that tends to be organized as a power law in the particle charge-to-mass ratio, Q/M. The power law exponent varies from event to event. As discussed by Leske et al. [9], this implies a correlation between variations of different isotope ratios that can be calculated with no free parameters if one adopts the reasonable assumption that isotopes of the same element have the same ionic charge state distribution. With this assumption the correlation depends only on the known mass ratios.

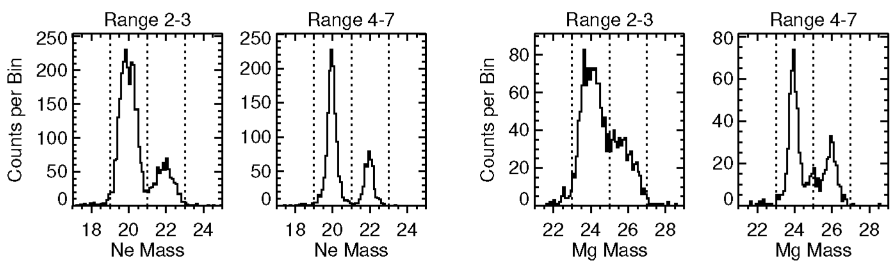

FIGURE 1. Mass histograms for Ne (left two panels) and Mg (right two panels) from ACE/SIS for the 20 Aug 2002 ^{3}He-rich SEP event. For these elements, range 2–3 corresponds to energies ~15–25 MeV/nuc and range 4–7 to ~25–110 MeV/nuc. Dotted lines indicate mass cuts used for deriving the ^{22}Ne/^{20}Ne and ^{26}Mg/^{24}Mg ratios used in this study.

In Figure 2 we compare the isotope ratios we measure in ^{3}He-rich events (open circles) with those reported for gradual events ($\times$ symbols, from [9]) and with the expected fractionation (dash-dot line) assuming power law dependence on Q/M and assuming that coronal/solar wind material (composition indicated by the dashed lines) provides the seed population on which the fractionation is imposed. We have included only those gradual events having relative uncertainties of 25% or less in both isotope ratios (45 of the 49 events used in [9]). For the ^{3}He-rich events, which tend to have much lower intensities, we have included the 15 events (from our overall list of 26) for which we have at least 3 counts for each of the four nuclides needed to make the plot. The ^{3}He-rich-event points are plotted with areas inversely proportional to their statistical uncertainty to emphasize those that are most precisely measured. The filled circle shows the isotope ratios obtained by summing the data from the 11 events that did not have sufficient counts to be included individually.

The Mg mass distribution has been split into "^{24}Mg" and "^{26}Mg" with a simple cut at the nominal location of ^{25}Mg, so both of the Mg isotopes should include a contribution of approximately 1/2 of the ^{25}Mg present in the event. Since the correlation between ^{25}Mg/^{24}Mg and ^{22}Ne/^{20}Ne is weaker than that between ^{26}Mg/^{24}Mg and ^{22}Ne/^{20}Ne, this admixture of ^{25}Mg alters the slope of the expected correlation, in addition to modifying the Mg isotope ratio assumed to represent the source composition that is being fractionated. The result is the dotted line, which shows the expected correlation including the ^{25}Mg admixtures and does not differ greatly from the dash–dot line.

A large fraction the gradual event isotope ratios are clustered around the point corresponding to solar wind composition. In cases where there are significant differences from solar wind composition, there is a tendency for the Ne and Mg isotope ratios to exhibit the expected correlation. The points for the ^{3}He-rich events are more scattered, but those measured with the best statistical accuracy do tend to fall near the predicted correlation line. Most of the events with poorer statistics fall below the calculated correlation line (i.e., have lower ^{26}Mg/^{24}Mg than predicted by the fractionation model based on the observed ^{22}Ne/^{20}Ne). While this might be due the large uncertainties in those measurements, it may also indicate a difference in the fractionation between the less-intense and the more-intense events. However, the fact that the summed data point from the smallest events (filled circle) does not deviate greatly from the predicted trend would cast doubt on an interpretation based on event intensity.

The presence of abundance enhancement trends that apparently can be organized as power laws in Q/M for both gradual and ^{3}He-rich SEP events suggests that there should be some features of the underlying acceleration processes that are common to the two types of events. For example, if the typically-small CMEs seen in some ^{3}He-rich events are sufficient to cause a second stage of acceleration, then in such events particles might exhibit the same sort of power-law in Q/M fractionation characteristic of the gradual events, in which the acceleration is attributed to CME-driven shocks (see also [9]). Leske et al. [10] looked for solar activity at the times of some of the most intense ^{3}He-rich events included in the present study and found possible CME associations with several of the events. A related issue concerns the Q/M-dependent spectral roll-offs observed in gradual events [11]. Since it is not uncommon for ^{3}He-rich event spectra to drop off faster than a power law at high energies [12], this phenomenon may affect composition in some ^{3}He-rich events and cause deviations from the expected trends.

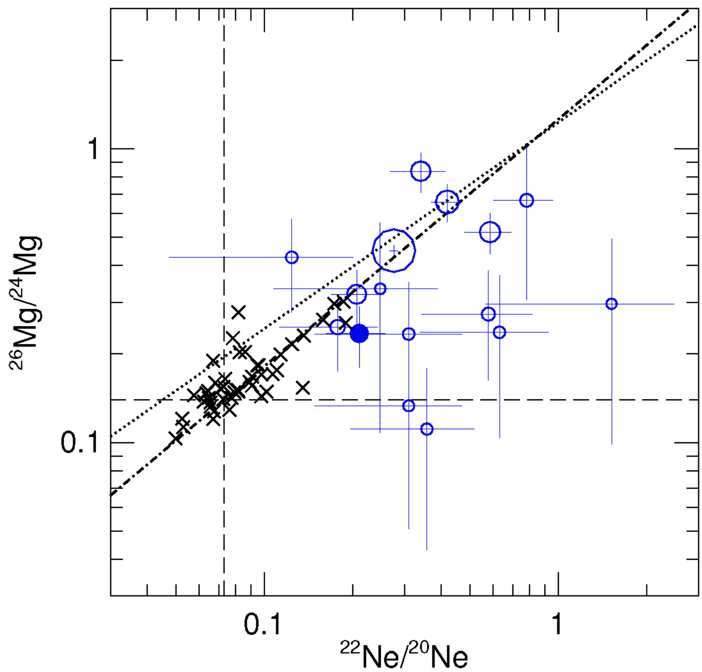

FIGURE 2. Correlation between between Mg and Ne isotope ratios measured in ^{3}He-rich events (open circles) compared with similar measurements in large, gradual SEP events ($\times$ symbols) [9]. The filled circle shows data from the sum of our 11 smallest ^{3}He-rich events. The points for ^{3}He-rich events are plotted with areas inversely proportional to the statistical uncertainties in the measurements to emphasize the more precisely determined points. Dashed lines indicate solar wind ratios. Dotted and dashed-dot lines show, respectively, the expected correlations with and without a ^{25}Mg admixture (see text).

It should be noted that nearly all of the ^{3}He-rich events shown in Figure 2 have higher ^{22}Ne/^{20}Ne ratios than all of the gradual events from [9]. Similarly, the enhancements of ^{26}Mg/^{24}Mg tend be larger in the more-intense ^{3}He-rich events than in the gradual events. In an earlier study, Dwyer et al. [13] investigated Ne and Mg isotopic composition at energies $<$3 MeV/nuc in SEP events having a wide range of ^{3}He/^{4}He ratios. They found that, on average, ^{22}Ne/^{20}Ne and ^{26}Mg/^{24}Mg increase with increasing ^{3}He/^{4}He, reaching $\sim$3–8$\times$ the solar wind values for ^{3}He-rich events with ^{3}He/^{4}He$\gtrsim$0.1. A number of the events in the present study have isotope enhancements that fall in this same range, but with some of the events having even larger enhancements of ^{22}Ne/^{20}Ne and with some of the smaller events having ^{26}Mg/^{24}Mg less enhanced.

ELEMENTAL COMPOSITION

Figure 3 shows the ^{3}He-rich-event elemental abundances (points with statistical uncertainties) relative to two different compositions thought to be representative of the solar

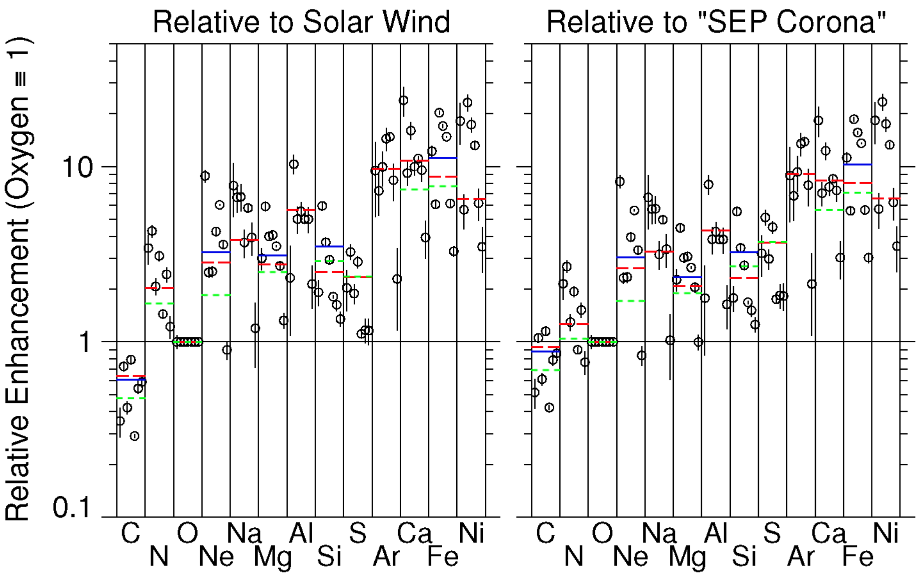

FIGURE 3. Abundance enhancements relative to solar wind composition in 7 ^{3}He-rich SEP events (points). Horizontal bars show average composition values reported in previous studies of ^{3}He-rich SEP events: solid, Mason et al. 1986 [15]; long dashes, Reames 1995 [14]; short dashes, Mason et al. 2004 [5]. In the left panel enhancements are shown relative to solar wind composition [3, 16], in the right panel relative to coronal composition inferred from gradual SEP event composition [14, 1].

corona. Points are included for the seven ^{3}He-rich events having the most statistically-precise heavy element abundance determinations. Also plotted as horizontal lines are the average impulsive flare event abundance enhancements from three different compilations: Reames 1995 ([14], long dashes), Mason et al. 2004 ([5], short dashes), and Mason et al. 1986 ([15], solid lines). Comparisons made in these earlier works with coronal composition were based on estimates of the latter abundances derived from measurements of gradual SEP events (see, for example, [14]), as done in the right panel of Figure 3, because direct measurements of coronal or solar wind abundances were not available for many of the elements. As a result of recent solar wind composition measurements, it is now possible to directly compare all of these abundances in ^{3}He-rich SEP events with those in the solar wind [3, 16]. This comparison is shown in the left panel. In both panels the abundance enhancements have been normalized to yield oxygen≡1.

Although there is event-to-event scatter of up to a factor ~10 (typically much larger than the measurement uncertainties) in some of the derived enhancement factors relative to oxygen, the present data generally reflect the same trends seen in the previous compilations of ^{3}He-rich SEP event composition. All of these earlier compilations were based on measurements at a few MeV/nuc or below, as compared with the 12–60 MeV/nuc energy range used for the composition results reported here. We see no clear indication of an energy dependence in the average composition of ^{3}He-rich SEP events.

If one assumes that abundance enhancements in ^{3}He-rich events should be monotonically increasing with Z [4, 5], a few elements stand out in Figure 3 as possible exceptions. The N abundance tends to have a larger enhancement than either C or O, and similarly the enhancement of Al tends to be greater than that of either Mg or Si.

DISCUSSION

The Z dependence of the abundance enhancements is generally thought to arise from a physical dependence on the mean Q/M values of the elements, which tend to decrease with increasing Z. The elemental and isotopic composition observations discussed in the preceding sections exhibit some patterns consistent with a smooth dependence of fractionation on Q/M. However there are indications that such a simple fractionation pattern applicable over a broad range of Q/M values may not represent the data in ^{3}He-rich events as well as it does in gradual events [9]. Specifically, we have noted deviations of the enhancements of some specific elements (e.g., N, Al) from the values expected from interpolation between neighboring elements (Figure 3). There are cases where $\langle Q/M \rangle$ from a thermal distribution is not a strictly monotonic function of Z (e.g., $\langle Q/M \rangle_{\mathrm{N}} < \langle Q/M \rangle_{\mathrm{O}} < \langle Q/M \rangle_{\mathrm{C}}$ just above 1 MK), but such cases tend to be restricted to narrow ranges of temperatures and of Z and thus seem unlikely to provide an explanation for the observations.

Wiedenbeck et al. [17] attempted to empirically fit SIS composition observations in several of the largest ^{3}He-rich events assuming fractionation of a underlying thermal population by a combination of power law and Gaussian functions of Q/M. Although these fits yielded better χ^2 values than a power law alone, large event-to-event variation of the best-fit parameters suggested a lack of physical basis for these fits.

Mullan [18, 19] considered a model in which fractionation is due to differences in the extent to which different ions are preaccelerated during the collapse of magnetic neutral sheets associated with a reconnection region. In this model, differences arise depending on whether the Coulomb collision energy-loss time scale for a particular ion ($\propto M/Q^2$) is less than or greater than the collapse time scale. It was found [19] that in this model ^{22}Ne/^{20}Ne tends to have the largest isotopic enhancement and may or may not be accompanied by a significant enhancement of ^{26}Mg/^{24}Mg. In addition, elemental abundance enhancements were found to have peaks in the ranges Mg–P and Cr–Fe but dips for C–N and S–Ar [18]. Such non-monotonic enhancement patterns bear some qualitative similarity to the composition found in ^{3}He-rich SEP events, suggesting that it may be useful to reexamine models of this type.

Direct measurements of ionic charge states in a number of ^{3}He-rich SEP events show a sharp rise in the mean charge of Fe, $\langle Q_{\mathrm{Fe}} \rangle$, in the energy range ~0.2–0.5 MeV/nuc (see [20] and references therein), indicating that stripping processes are important for establishing the observed charged states. An acceleration site in the low corona was inferred based on the matter density needed for Coulomb collisions to cause the necessary stripping on the time scale of the particle acceleration. Detailed models of charge state formation and transport in ^{3}He-rich events (see [21] and references therein) indicate that a range of source temperatures may be required and that adiabatic deceleration plays a significant role in establishing the observed energy dependence of $\langle Q_{\mathrm{Fe}} \rangle$.

Several studies correlating ^{3}He-rich SEP events detected near 1 AU with imaging observations of their solar source regions [22, 23, 24] have shown that coronal jets are present in some of these events. It remains to be established whether the bulk flows indicated by these jets play a role in the particle acceleration (as do CMEs in gradual SEP events) or are merely a consequence of the reconnection between flare loops and open magnetic field lines that allows accelerated ions to escape into the interplanetary medium.

The wealth of observations, both in situ and remote sensing, now being obtained for ^{3}He-rich SEP events are providing new insights into the physical origin of these events. Further investigation of ^{3}He-rich events during the coming solar maximum should lead to major advances in this area.

ACKNOWLEDGMENTS

This research was supported by NASA at the California Institute of Technology (grant NAG5-12929), the Jet Propulsion Laboratory, and the Goddard Space Flight Center

REFERENCES

1. D. V. Reames, *Space Science Reviews* **90**, 413 (1999).
2. G. M. Mason, *Space Science Reviews* **130**, 231 (2007).
3. P. Bochsler, *Astronomy and Astrophysics Review* **14**, 1 (2007).
4. D. V. Reames, and C. K. Ng, *Astrophysical Journal* **610**, 510 (2004).
5. G. M. Mason, et al., *Astrophysical Journal* **606**, 555 (2004).
6. P. Mazzotta, et al., *Astronomy and Astrophysics Supplement Series* **133**, 403 (1998).
7. E. C. Stone, et al., *Space Science Reviews* **86**, 357 (1998).
8. H. H. Breneman, and E. C. Stone, *Astrophysical Journal (Letters)* **299**, L57 (1985).
9. R. A. Leske, et al., *Space Science Reviews* **130**, 195 (2007).
10. R. A. Leske, et al., *28th International Cosmic Ray Conference (Durban)* **6**, 3253 (2003).
11. C. M. S. Cohen, et al., *Advances in Space Research* **32**, 2649 (2003).
12. G. M. Mason, et al., *Astrophysical Journal* **574**, 1039 (2002).
13. J. R. Dwyer, et al., *Astrophysical Journal* **563**, 403 (2001).
14. D. V. Reames, *Advances in Space Research* **15**, 41 (1995).
15. G. M. Mason, et al., *Astrophysical Journal* **303**, 849 (1986).
16. R. Karrer, et al., *Space Science Reviews* **130**, 317 (2007).
17. M. E. Wiedenbeck, et al., *28th International Cosmic Ray Conference (Durban)* **6**, 3245 (2003).
18. D. J. Mullan, and R. H. Levine, *Astrophysical Journal Supplement* **47**, 87 (1981).
19. D. J. Mullan, *Astrophysical Journal* **268**, 385 (1983).
20. B. Klecker, et al., *Space Science Reviews* **130**, 273 (2007).
21. Y. Y. Kartavykh, et al., *Astrophysical Journal* **671**, 947 (2007).
22. Y.-M. Wang, et al., *Astrophysical Journal* **639**, 495 (2006).
23. N. V. Nitta, et al., *Astrophysical Journal* **650**, 438 (2006).
24. N. V. Nitta, et al., *Astrophysical Journal (Letters)* **675**, L125 (2008).